

## 12

# From neutral currents to weak vector bosons

*The unification of weak and electromagnetic interactions, 1973–1987*

Fermi's theory of weak interactions survived nearly unaltered over the years. Its basic structure was slightly modified by the addition of Gamow-Teller terms and finally by the determination of the V-A form, but its essence as a four fermion interaction remained. Fermi's original insight was based on the analogy with electromagnetism; from the start it was clear that there might be vector particles transmitting the weak force the way the photon transmits the electromagnetic force. Since the weak interaction was of short range, the vector particle would have to be heavy, and since beta decay changed nuclear charge, the particle would have to carry charge. The weak (or W) boson was the object of many searches. No evidence of the  $W$  boson was found in the mass region up to 20 GeV.

The V-A theory, which was equivalent to a theory with a very heavy  $W$ , was a satisfactory description of all weak interaction data. Nevertheless, it was clear that the theory was not complete. As described in Chapter 6, it predicted cross sections at very high energies that violated unitarity, the basic principle that says that the probability for an individual process to occur must be less than or equal to unity. A consequence of unitarity is that the total cross section for a process with angular momentum  $J$  can never exceed  $4\pi(2J + 1)/p_{cm}^2$ . However, we have seen that neutrino cross sections grow linearly with increasing center of mass energy. When the energy exceeds about 300 GeV, there would be a contradiction.

It might be hoped that the theory could be calculated more completely, to a higher order in the Fermi coupling constant. In a complete theory, these corrections could bring the predictions back into the allowed range. Unfortunately, the Fermi theory cannot be calculated to higher order because the results are infinite. Infinities arise in calculating quantum electrodynamics (QED) to higher order, as well. In QED, it is possible to absorb these infinities so that none appears in the physical results. This is impossible in the Fermi theory. Writing the Fermi theory

in terms of the  $W$  bosons enhances the similarity with QED, but the infinities remain.

The first step in the solution to this problem came from C. N. Yang and R. Mills, who in 1954 developed a theory of massless interacting vector particles. This theory could accommodate particles like the photon,  $W^+$ , and  $W^-$  that would interact with one another, but it required them to be massless. The infinities in the model could be reabsorbed (the model was “renormalizable”). An important advance was made by Peter Higgs, who in 1964 showed how a theory initially containing a massless photon and two scalar particles could turn into a theory with a massive vector particle and one scalar. This “Higgs mechanism” was a key ingredient in the final model.

The standard model of electroweak interactions, developed largely by Glashow, Weinberg, and Salam begins with massless Yang–Mills particles. These are denoted  $W^+$ ,  $W^-$ ,  $W^0$ , and  $B$  (not to be confused with the  $B$  meson of the previous chapter, which plays no role here). The  $W$ s form a triplet of a new symmetry, “weak isospin”, while the  $B$  is an isosinglet. The Higgs mechanism is invoked to give mass to the  $W$  bosons. At the same time, the two neutral particles,  $W^0$  and  $B$  mix to produce two physical particles, the photon (represented by the field  $A$ ) and the  $Z$ . The photon, of course, is massless. The  $Z$  acquires a mass comparable to that of the  $W$ .

The Fermi theory is equivalent to the exchange of only charged weak bosons. This allows for processes like  $\nu_\mu e^- \rightarrow \mu^- \nu_e$ , which may be viewed as emission of a  $W^+$  by the initial neutrino, which turns into a muon and its absorption by the electron, which turns into an electron-neutrino. When the  $W$  is emitted or absorbed, the charges of the interacting particles are changed. The currents to which the  $W$  attaches, for example  $\bar{e}\gamma_\mu(1-\gamma_5)\nu$ , are called charged currents. The process  $\nu_\mu e^- \rightarrow \nu_\mu e^-$  cannot proceed in the Fermi theory because the charged current can change  $\nu_\mu$  only to  $\mu^-$ , not to  $e^-$ , as was shown by the two-neutrino experiment discussed in Chapter 7. The  $Z$  boson adds new interactions, ones with neutral currents. The  $\nu_\mu$  can emit a  $Z$  which is absorbed by the electron, thus permitting the process  $\nu_\mu e^- \rightarrow \nu_\mu e^-$ . No charge is transferred. The existence of weak neutral currents is a dramatic prediction of the model.

In fact, neutral-current processes had been searched for in decays like  $K^+ \rightarrow \pi^+ e^- e^+$  and  $K_L^0 \rightarrow \mu^+ \mu^-$  (where the  $e^+ e^-$  or  $\mu^+ \mu^-$  would be viewed as coming from a virtual  $Z$ ) and found to be very rare or nonexistent. These searches had been limited invariably to strangeness-changing neutral currents, for example the current that transformed a  $K^+$  into a  $\pi^+$ . The reason for this limitation was simple. In most instances where there is no change of strangeness, if a  $Z$  can be exchanged, so can a photon. Thus the effect of the  $Z$ , and hence of the neutral weak current, was always masked by a much larger electromagnetic effect. One way to avoid this was to look for scattering initiated by a neutrino that emitted a  $Z$  that subsequently interacted with a nuclear target. This process

could not occur electromagnetically since the neutrino does not couple to photons. The signature of such a process was the absence of a charged lepton in the final state.

Although neutral currents were predicted in the model of Glashow, Weinberg, and Salam, the intensity of the search for them increased dramatically in the early 1970s when, through the work of G. 't Hooft and others, the theory was shown to be renormalizable. Weinberg and Salam had conjectured that the theory was renormalizable, but there was no proof initially.

The discovery of neutral-weak-current interactions was made in mid-1973 by A. Lagarrigue, P. Musset, D. H. Perkins, A. Rousset and co-workers using the Gargamelle bubble chamber at CERN (**Ref. 12.1**). The experiment used separate neutrino and antineutrino beams. The beams were overwhelmingly muon-neutrinos, so the task was to demonstrate the occurrence of events without a final-state muon. Muons could be distinguished from hadrons in the bubble chamber because it was filled with a rather dense material, freon, in which most of the produced hadrons would either interact or range out. The muons, then, were signaled by the particles exiting from the chamber without undergoing a hadronic interaction.

The background with the greatest potential to obscure the results was due to neutrino interactions occurring in the shielding before the bubble chamber. Neutrons produced in these interactions could enter the bubble chamber without leaving a track and cause an event from which, of course, no muon would emerge. The Gargamelle team was able to control this background by studying a related class of events. Some ordinary charged-current events occurring within the bubble chamber yielded neutrons that subsequently had hadronic collisions inside the bubble chamber. These events were quite analogous to the background events in which the initial neutrino interaction took place in the shielding. By studying the events in which the neutron's source was apparent, it was possible to place limits on the neutron background arising outside the chamber. In addition, the neutral-current events had another characteristic that indicated they were due to neutrinos. They were evenly distributed along the length of the bubble chamber. If they had come from neutrons there would have been more of them at the front and fewer at the back as a consequence of the depletion of the neutrons traveling through the freon. The neutrinos have such a small cross section that there is no measurable attenuation.

Not only did the experiment find convincing evidence for the neutral-current events, it measured the ratio of neutral-current to charged-current events both for neutrinos and antineutrinos. This was especially important because it provided a means of measuring the value of the neutral weak charge to which the  $Z$  boson coupled.

The electroweak theory contains three fundamental parameters aside from the masses of the particles and the mixing angles in the Kobayashi-Maskawa matrix.

Once these are determined, all purely electroweak processes can be predicted. To determine the three parameters, it is necessary to measure three fundamental quantities. There is, however, a great deal of freedom in choosing these experimental quantities. It is natural to take two of them to be  $\alpha_{em} \approx 1/137$  and  $G_F \approx 1.166 \cdot 10^{-5} \text{ GeV}^{-2}$  since these are quite well measured. The third quantity must involve some new feature introduced by the electroweak model. The strength of the neutral weak currents is such a quantity. The result is often expressed in terms of the weak mixing angle  $\theta_W$  that indicates the degree of mixing of the  $W^0$  and  $B$  bosons that generates the photon and  $Z$ :

$$\begin{aligned} A &= \sin \theta_W W^0 + \cos \theta_W B; & W^0 &= \sin \theta_W A + \cos \theta_W Z; \\ Z &= \cos \theta_W W^0 - \sin \theta_W B; & B &= \cos \theta_W A - \sin \theta_W Z. \end{aligned}$$

The photon couples to particles according to their charges. We can represent the coupling to a fermion  $f$  by

$$\bar{f} \gamma_\mu e Q f A^\mu$$

or, in shorthand,  $eQA$ , where  $Q$  measures the charge of a particle in units of the proton charge,  $e$ , and  $A$  is the electromagnetic vector potential.

The absorption of a  $W^+$  boson changes an electron into a neutrino. This action can be represented by the isospin operator  $T_+$  if the neutrino and electron form a doublet with the neutrino being the  $T_3 = 1/2$  component. Of course, we already know that it is only the left-handed component of the electron that participates, so we assign zero weak isospin to the right-handed part of the electron. The quarks are treated analogously, with the absorption of a  $W^+$  changing a left-handed  $d$  into a left-handed  $u$ .

The  $B$  boson couples to fermions according to another new quantum number, the “weak hypercharge”,  $Y$ . These new quantum numbers satisfy an analog of the Gell-Mann–Nishijima relation  $Q = T_3 + Y/2$  as shown in Table 12.1.

|                |       |       |         |       |       |       |       |
|----------------|-------|-------|---------|-------|-------|-------|-------|
|                | $e_L$ | $e_R$ | $\nu_L$ | $u_L$ | $u_R$ | $d_L$ | $d_R$ |
| $Q$            | -1    | -1    | 0       | 2/3   | 2/3   | -1/3  | -1/3  |
| $T_3$          | -1/2  | 0     | 1/2     | 1/2   | 0     | -1/2  | 0     |
| $\frac{1}{2}Y$ | -1/2  | -1    | -1/2    | 1/6   | 2/3   | 1/6   | -1/3  |

Table 12.1. The weak interaction quantum numbers of quarks and leptons in the standard model. The subscripts indicate left-handed and right-handed components.

After the mixing of the  $B$  and  $W^0$  that produces the photon and the  $Z$ , the coupling of the photon to fermions is given by  $eQ$  and that of the  $Z$  by

$$\frac{e}{\sin \theta_W \cos \theta_W} [T_3 - Q \sin^2 \theta_W]$$

where  $T_3$  has an implicit  $(1 - \gamma_5)/2$  included to project out the left-hand part of the fermion. This is explained in greater detail below. Because the  $Z$  couples differently to left-handed and right-handed fermions, its interactions are parity violating. By comparing the couplings of the  $Z$  to that of the  $W$ , it is possible to derive a relation for the ratio of neutral-current events to charged-current events in deep inelastic neutrino scattering,  $NC/CC$ , using the parton model discussed in Chapter 8. Although the parton model is expected to work best at very high energies, the early Gargamelle results on charged currents showed that the model worked well even at the low energies available to Gargamelle using the CERN Proton Synchrotron. If the scattering of the neutrinos from antiquarks is ignored (a 10–20% correction), the predictions are

$$R_\nu = \left( \frac{NC}{CC} \right)_\nu = \frac{1}{2} - \sin^2 \theta_W + \frac{20}{27} \sin^4 \theta_W$$

$$R_{\bar{\nu}} = \left( \frac{NC}{CC} \right)_{\bar{\nu}} = \frac{1}{2} - \sin^2 \theta_W + \frac{20}{9} \sin^4 \theta_W$$

In these relations, it is assumed that

$$M_Z^2 = M_W^2 / \cos^2 \theta_W$$

a prediction of the simplest version of the standard model of electroweak interactions as discussed below. The Gargamelle results indicated that  $\sin^2 \theta_W$  was in the range 0.3 to 0.4.

These results were followed by confirmation from other laboratories. The neutral-current events were not rare. They were easy to find. The problem was to demonstrate that they were not due to any of the various backgrounds. The Harvard–Penn–Wisconsin (HPW) experiment at Fermilab did verify the result, but only after some considerable difficulty in determining their efficiency for identifying muons (Ref. 12.2). The HPW experiment was a counter experiment. The target and detector were combined into a segmented unit. This was followed by a muon spectrometer. A diagram of the apparatus and the appearance of an event in the detector are shown in Figure 12.52. Inevitably there was the problem of determining how many muons failed, for geometrical reasons, to enter the muon spectrometer.

Another Fermilab experiment, a Caltech–Fermilab collaboration, also confirmed the existence of neutral currents (Ref. 12.3). A good measurement of  $\sin^2 \theta_W$ , however, had to await the results of the CERN experiments, carried out by the CDHS, CHARM, and BEBC collaborations mentioned in Chapter 8. The CERN experiments used a beam from the Super Proton Synchrotron (SPS). The

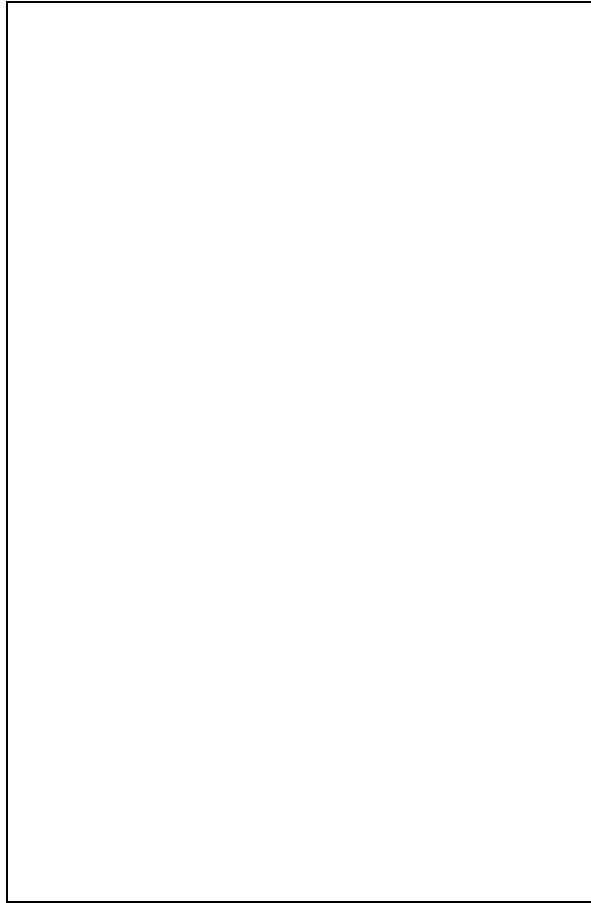


Figure 12.52: Diagram (a) of the HPW neutrino detector used at Fermilab (Ref. 12.2). There were eight spark chambers (SC) and sixteen liquid scintillator segments. The muon spectrometer contained four magnetized iron toroids. Additional scintillator counters are labeled  $A, B, C, D$ . An event is seen in the spark chambers and the same event is shown enlarged in (b). A muon track is visible in the muon spectrometer so this is a charged current event. The energy deposition for the event is displayed in (c).

values obtained were about 0.30 for  $R_\nu$  and 0.38 for  $R_{\bar{\nu}}$ . More recent analyses of the neutral-current data find a value  $\sin^2 \theta_W = 0.23$ .

The existence of the neutral currents was important circumstantial evidence for the electroweak model. The neutral-current to charged-current ratios lay close to the curve required by the model. Very impressive evidence came from a different kind of neutral-current experiment performed at SLAC. This experiment measured the interference between an electromagnetic amplitude and one due to neutral weak currents.

The experiment of Prescott and co-workers (**Ref. 12.4**) measured the scattering of longitudinally polarized electrons from a deuterium target. A dependence of the cross section on the value of  $\boldsymbol{\sigma}_e \cdot \mathbf{p}_e$ , where  $\boldsymbol{\sigma}_e$  is the electron's spin, is necessarily a parity violation since this is a pseudoscalar quantity. The experiment actually measured the asymmetry

$$A = \frac{\sigma_R - \sigma_L}{\sigma_R + \sigma_L}$$

where the subscript on the cross section indicates a right-handed or left-handed electron incident.

The right-handed and left-handed electron beams were produced by a source using a laser shining on a GaAs crystal. A Pockels cell allowed linearly polarized laser light to be changed into circularly polarized light, with the polarization changed pulse to pulse in a random way, which was recorded. The polarized photons ejected polarized electrons from the crystal, with an average polarization of 37%.

On the basis of very general considerations, it was possible to see that the weak-electromagnetic interference effect should give  $A$  a value of order  $G_F Q^2 / \alpha$  where  $Q^2$  is the momentum transferred squared of the electron (and is not to be confused with the charge operator!). A more complete calculation shows the effect ought to be about one-tenth this size, or near  $10^{-4}$  for  $Q^2$  of about  $1 \text{ GeV}^2$ . In order that such an effect not be masked by statistical fluctuations, about  $10^{10}$  events are needed. This was achieved by integrating outputs of phototubes rather than counting individual events.

The scattered electrons were collected in a magnetic spectrometer like that used in the pioneering deep inelastic scattering experiments carried out 10 years before. Measurements were made for several beam energies. Because the beam was bent through an angle of  $24.5^\circ$  before scattering, the polarized electrons precessed. This provided an additional check of the measurements.

The asymmetry can be predicted within the standard electroweak model. The result is a function of  $y = (E - E')/E$ , the fraction of the incident electron's energy that is lost:

$$A = \frac{-G_F Q^2}{2\sqrt{2}\pi\alpha} \frac{9}{10} \left\{ 1 - \frac{20}{9} \sin^2 \theta_W + (1 - 4 \sin^2 \theta_W) \left[ \frac{1 - (1 - y)^2}{1 + (1 - y)^2} \right] \right\}$$

The result of the experiment,  $A/Q^2 = (-9.5 \pm 1.6) \times 10^{-5} \text{ GeV}^{-2}$ , was in good agreement with the standard model for a value  $\sin^2 \theta_W = 0.20 \pm 0.03$ . The measurement of the weak mixing angle in the neutral-current experiments made it possible to predict the masses of the  $W$  and  $Z$ .

Masses arise in the standard model from the Higgs mechanism, which is due to hypothetical scalar particles, known as Higgs particles. The field corresponding to a neutral Higgs particle obtains a vacuum expectation value that is nonzero because this minimizes the energy of the vacuum. The various massless particles in the theory obtain masses by interacting with this ubiquitous nonzero field. The coupling of the vector (gauge) particles is governed by the analog of the usual minimal coupling of electrodynamics:

$$D_\mu = \partial_\mu - ieQA_\mu$$

In the conventional model, the Higgs particle is part of a complex isodoublet. This is analogous to the kaon multiplet. There are four states, two charged and two neutral. We can represent this as a two component vector

$$\begin{pmatrix} \phi^+ \\ \phi^0 \end{pmatrix}$$

and its complex conjugate. In the vacuum, the field  $\phi^0$  is nonzero:  $\langle \phi^0 \rangle = v/\sqrt{2}$ . The analog of the minimal coupling is

$$D_\mu = \partial_\mu - ig\mathbf{T} \cdot \mathbf{W}_\mu - ig'(Y/2)B_\mu$$

where the three components of  $\mathbf{T}$  are the generators of the weak isospin and where  $g$  and  $g'$  are two coupling constants, one for  $SU(2)$  and one for  $U(1)$ . Rewritten in terms of the physical particles, this is

$$D_\mu = \partial_\mu - ieQA_\mu - ig(T_+W_\mu^+ + T_-W_\mu^-)/\sqrt{2} - ig(T_3 - \sin^2\theta_W Q)Z_\mu/\cos\theta_W$$

The relations between  $e, g, g'$ , and  $\theta_W$  are

$$\tan\theta_W = \frac{g'}{g}, \quad 1/g^2 + 1/g'^2 = 1/e^2$$

A comparison with the usual V-A theory shows that

$$\frac{G_F}{\sqrt{2}} = \frac{g^2}{8M_W^2}$$

This determines the  $W$  mass :

$$M_W^2 = \frac{\pi\alpha}{\sqrt{2}\sin^2\theta_W G_F}$$

In fact, a more precise result is obtained by using the electromagnetic coupling measured not at zero momentum transfer but rather at a momentum squared equal to  $M_W^2$ ,  $\alpha(M_W^2) \approx 1/128$ , a value that takes into account vacuum polarization corrections. Inserting the vacuum expectation value of the Higgs field we find mass terms from

$$(D_\mu\phi)^\dagger D_\mu\phi \rightarrow \frac{1}{2} \left[ \frac{g^2 v^2}{4} (W_\mu^+ W^{-\mu} + W_\mu^- W^{+\mu}) + \frac{g^2 v^2}{4 \cos^2 \theta_W} Z_\mu Z^\mu \right]$$

This gives for the  $Z$  mass

$$M_Z^2 = M_W^2 / \cos^2 \theta_W$$

and with  $\sin^2 \theta_W = 0.23$ ,  $M_W = 80$  GeV,  $M_Z = 92$  GeV.

With a promising theory and a good measurement of  $\sin^2 \theta_W$ , the search for the  $W$  and  $Z$  now took a different character. The masses could be predicted from the results of the neutral-current measurements of  $\sin^2 \theta_W$  and lay outside the range of existing machines. Following a proposal by D. Cline, C. Rubbia, and P. McIntyre, a major effort at CERN, led by C. Rubbia and S. van der Meer, transformed



the SPS into a colliding beam machine, the Sp $\bar{p}$ S. The regular proton beam was used to create antiprotons, which were captured and stored. The antiprotons then re-entered the SPS, but moving in the opposite direction. A particularly difficult problem was to compress the beam of antiprotons so that it would be dense enough to cause many collisions when the protons moving the other way passed through it.

If a  $u$  quark from a proton and an  $\bar{d}$  quark from an antiproton collided, a  $W^+$  could be created if the energy of the pair were near the mass of the  $W$ . The  $W^+$  would decay into  $e^+\nu$  about 8% of the time. The cross section for this process was calculated to be a fraction of a nanobarn ( $10^{-33}\text{cm}^2$ ). A more spectacular signal could be obtained from  $Z$ s that decayed into  $e^+e^-$  or  $\mu^+\mu^-$ .

The  $W$  and  $Z$  bosons were discovered by the two large collaborations, UA-1 (Ref. 12.5) and UA-2 (Ref. 12.6), working at the Sp $\bar{p}$ S Collider. The UA-1 detector used a uniform magnetic field of 0.7 T (7 kG) perpendicular to the beam. Inside the field was a high quality drift chamber. External to the drift chamber was extensive coverage by electromagnetic and hadronic calorimeters. The critical capability of discriminating between electrons and hadrons was achieved using many radiation lengths of material, segmented into layers. By covering nearly all of the full  $4\pi$  steradians with calorimetry, it was possible to check momentum balance in the plane perpendicular to the beam. This, in effect, provided a neutrino detector for those neutrinos with transverse momentum above 15 GeV or so.

In colliding-beam machines like SPEAR, DORIS, PETRA, PEP, ISR, and the Sp $\bar{p}$ S Collider, the event rate is related to the cross section by

$$\text{Rate} = \mathcal{L}\sigma$$

where  $\mathcal{L}$  is the luminosity and is measured in  $\text{cm}^{-2}\text{s}^{-1}$ . The luminosity depends on the density of the intersecting beams and their degree of overlap. The total number of events is  $\sigma \int \mathcal{L}dt$ . For the results reported by UA-1,  $\int \mathcal{L}dt = 18\text{nb}^{-1}$  at an energy of  $\sqrt{s} = 540\text{GeV}$ . The total event rate was high so various triggers were used to choose the small subset of events to be recorded.

Events with electron candidates that had high transverse momentum detected in the central part of the calorimeter and that were well-separated from any other high transverse momentum particles were selected. This class contained 39 events. Five of these contained no hadronic jets and thus had a significant transverse momentum imbalance, as would be expected for decays  $W \rightarrow e\nu$ . An alternative search through the same recorded events sought those with large momentum imbalance. The same five events were ultimately isolated, together with two additional events that were candidates for  $W \rightarrow \tau\nu$ .

The mass of the  $W$  could be estimated from the observed transverse momenta. The result was  $M_W = 81 \pm 5\text{GeV}$ , in good agreement with predictions of the standard model using the weak mixing angle as measured in neutral-current experiments. Similar results were obtained by the UA-2 collaboration and also by

observing the muonic decay of the  $W$  (Ref. 12.7)

Later, the two collaborations detected the  $Z$  through its decays  $Z \rightarrow e^+e^-$  (Refs. 12.8, 12.9) and  $Z \rightarrow \mu^+\mu^-$  (Ref. 12.10). This discovery took longer because the cross section for  $Z$  production is somewhat smaller than that for  $W$ s and because the branching ratios  $Z \rightarrow e^+e^-$  and  $Z \rightarrow \mu^+\mu^-$  are expected to be only 3% each, while  $W \rightarrow e\nu$  and  $W \rightarrow \mu\nu$  should be 8% each. However, the signature of two leptons with large invariant mass was unmistakable, and only a few events were necessary to establish the existence of the  $Z$  with a mass consistent with the theoretical expectation. An event that is a  $Z^0$  candidate measured by the UA-1 Collaboration is shown in Figure 12.53. The lego plots for four UA-1  $Z^0$  candidates are shown in Figure 12.54. An event measured by the UA-2 Collaboration is shown in Figure 12.55, together with its lego plot. During running at an increased center-of-mass energy of 630 GeV additional data were accumulated. Results for the decay  $Z \rightarrow e^+e^-$  obtained by the UA-1 and UA-2 Collaborations are shown in Figure 12.56.

The discovery of the  $W$  and the  $Z$  dramatically confirmed the electroweak theory. Its unification of the seemingly unrelated phenomena of nuclear beta decay and electromagnetism is one of the major achievements of twentieth century physics. There are no important data on electroweak interactions that are in conflict with the theory. With elegance and simplicity, it subsumes the phenomenological V-A theory, extends that theory to include neutral current phenomena and meets the theoretical demand of renormalizability. The unification of electromagnetism and weak interactions is a fitting conclusion to the search for a weak interaction theory, which began with Fermi's prescient observation that the fundamental process of beta decay,  $n \rightarrow pe\nu$  might be viewed as the interactions of two currents.

Figure 12.53: A UA-1 event display for a candidate for  $Z^0 \rightarrow e^+e^-$ . (a) Display of reconstructed tracks and calorimeter hits. (b) Display of tracks with  $p_T > 2$  GeV/c and calorimeter hits with  $E_T > 2$  GeV. The electron pair emerges cleanly from the event (Ref. 12.8).

Figure 12.54: Lego plots for four UA-1 events that were candidates for  $Z^0 \rightarrow e^+e^-$ . The plots show the location of energy deposition in  $\phi$ , the azimuthal angle, and  $\eta = -\ln \tan(\theta/2)$ , the pseudorapidity. The isolated towers of energy indicate the cleanliness of the events (Ref. 12.8).

Figure 12.55: A UA-2 candidate for  $Z^0 \rightarrow e^+e^-$ . The upper diagram shows a track detected by a series of proportional chambers and a chamber following a tungsten converter. The calorimeter cells indicate energy measured by the electromagnetic calorimeter. The lego plot for the event shows two isolated depositions of electromagnetic energy, indicative of an  $e^+e^-$  pair (Ref. 12.9).

Figure 12.56: (a) The invariant mass distribution for  $e^+e^-$  pairs identified through electromagnetic calorimetry in the UA-1 detector. (Figure supplied by UA-1 Collaboration)  
(b) The analogous plot for the UA-2 data (Ref. 12.12). In both data sets, the  $Z$  appears well-separated from the lower mass background.

## EXERCISES

- 12.1 Make a graph with  $(NC/CC)_\nu$  as abscissa and  $(NC/CC)_{\bar{\nu}}$  as ordinate. Draw the curve of values allowed by the standard model ignoring contributions from antiquarks. Plot the results quoted in the text. What value of  $\sin^2 \theta_W$  do you find?
- 12.2 Derive the predictions for  $(NC/CC)_\nu$  and  $(NC/CC)_{\bar{\nu}}$  by comparing the couplings of the W:

$$gT_+/\sqrt{2} = eT_+/\sin \theta_W \sqrt{2}$$

and the Z:

$$e(T_3 - Q \sin^2 \theta_W)/\sin \theta_W \cos \theta_W$$

Use an isoscalar target. For  $|q|^2 \ll M_W^2, M_Z^2$ , the vector boson propagator is essentially  $1/M_W^2$  or  $1/M_Z^2$ .

- 12.3 Use relations analogous to those in Chapter 8 for  $e_L^- \mu_L^- \rightarrow e_L^- \mu_L^-, e_R^- \mu_L^-,$  etc. to derive the expression for the asymmetry,  $A$ , in polarized–electron deuteron scattering.
- 12.4 The classical equation for the motion of a charged particle with mass  $m$ , charge  $e$  and  $g$ -factor,  $g$ , in a plane perpendicular to a uniform field  $\mathbf{B}$  is

$$\frac{d\boldsymbol{\beta}}{dt} = \frac{e}{m\gamma} \boldsymbol{\beta} \times \mathbf{B}$$

where  $\boldsymbol{\beta}$  is the velocity vector ( J. D. Jackson, *Classical Electrodynamics*, 2nd Edition, Wiley, New York, 1975. p 559). If the direction of the spin is denoted  $\mathbf{s}$ , then

$$\frac{d\mathbf{s}}{dt} = \frac{e}{m} \mathbf{s} \times \left( \frac{g}{2} - 1 + \frac{1}{\gamma} \right) \mathbf{B}$$

Use these equations to verify the precession equation, Eq. (4) of Ref. 12.4.

- 12.5 \* Assume that the  $W$  production at the Sp $\bar{p}$ S Collider is due to the annihilation of a quark from the proton and an antiquark from the antiproton. Show that if the proton direction defines the  $z$  axis, the produced  $W$ s have  $J_z = -1$ . Show that in the  $W$  rest frame the outgoing negative leptons from  $W^- \rightarrow l^- \bar{\nu}$  have the angular distribution  $(1 + \cos \theta^*)^2$ , while the positive leptons from  $W^+ \rightarrow l^+ \bar{\nu}$  have the angular distribution  $(1 - \cos \theta^*)^2$ , where  $\theta^*$  is measured from the  $z$  (proton) direction. What is expected for  $Z$  decay? Compare with available data, e.g. S. Geer, in *Proceedings of the XXIII International Conference on High Energy Physics, Berkeley, 1986*, S. C. Loken ed., World Scientific, Singapore, 1987, p. 982.

## BIBLIOGRAPHY

Some of the same material is covered in D. H. Perkins *Introduction to High Energy Physics*, Addison-Wesley, Menlo Park, California, 1987, Chapter 8.

A more theoretical, but non-technical presentation is given by C. Quigg *Gauge Theories of the Strong, Weak, and Electromagnetic Interactions*, Benjamin/Cummings, Menlo Park, California, 1983.

The standard model is covered in E. D. Commins and P. H. Bucksbaum, *Weak Interactions of Leptons and Quarks*, Cambridge University Press, Cambridge, 1983.

A semi-popular account of the  $W$  and  $Z$  discoveries is given by P. Watkins, *Story of the  $W$  and  $Z$* , Cambridge University Press, New York, 1986.

## REFERENCES

- 12.1 F. J. Hasert *et al.*, "Observation of Neutrino-like Interactions without Muon or Electron in the Gargamelle Neutrino Experiment." *Phys. Lett.*, **46B**, 138 (1973).
- 12.2 A. Benvenuti *et al.*, "Observation of Muonless Neutrino-Induced Inelastic Interactions." *Phys. Rev. Lett.*, **32**, 800 (1974).
- 12.3 B. C. Barish *et al.*, "Neutral Currents in High Energy Neutrino Collisions: An Experimental Search." *Phys. Rev. Lett.*, **34**, 538 (1975).
- 12.4 C. Y. Prescott *et al.*, "Parity Non-Conservation in Inelastic Electron Scattering." *Phys. Lett.*, **77B**, 347 (1978).
- 12.5 UA 1 Collaboration, "Experimental Observation of Isolated Large Transverse Energy Electrons with Associated Missing Energy at  $\sqrt{s} = 540$  GeV." *Phys. Lett.*, **122B**, 103 (1983).
- 12.6 UA 2 Collaboration, "Observation of Single Isolated Electrons of High Transverse Momentum in Events with Missing Transverse Energy at the CERN  $\bar{p}p$  Collider." *Phys. Lett.*, **122B**, 476 (1983).
- 12.7 UA 1 Collaboration, "Observation of the Muonic Decay of the Charged Intermediate Vector Boson." *Phys. Lett.*, **134B**, 469 (1984).
- 12.8 UA 1 Collaboration, "Experimental Observation of Lepton Pairs of Invariant Mass around 95 GeV/ $c^2$  at the CERN SPS Collider." *Phys. Lett.*, **126B**, 398 (1983).



- 12.9 UA 2 Collaboration, "Evidence for  $Z^0 \rightarrow e^+e^-$  at the CERN  $\bar{p}p$  Collider." *Phys. Lett.*, **129B**, 130 (1983).
- 12.10 UA 1 Collaboration, "Observation of Muonic  $Z^0$  Decay at the  $\bar{p}p$  Collider." *Phys. Lett.*, **147B**, 241 (1984).
- 12.11 UA 1 Collaboration, "Recent Results on Intermediate Vector Boson Properties at the CERN Super Proton Synchrotron Collider." *Phys. Lett.*, **166B**, 484 (1986).
- 12.12 UA 2 Collaboration, "Measurements of the Standard Model Parameters from a Study of W and Z Bosons." *Phys. Lett.*, **186B**, 440 (1987).